Environ. Chem. **2014**, *11*, 333–340
doi:10.1071/EN13192_AC

Supplementary material

Effects of nitrate and humic acid on enrofloxacin photolysis in an aqueous system under three light conditions: kinetics and mechanism

Yang Li,[A] *Junfeng Niu,*[A,B] *Enxiang Shang,*[A] *Mengyuan Zheng*[A] *and Tianlai Luan*[A]

[A]State Key Laboratory of Water Environment Simulation, School of Environment, Beijing Normal University, Beijing 100875, P.R. China.

[B]Corresponding author. Email: junfengn@bnu.edu.cn

Photolysis experimental setup

Fig. S1 is a schematic of the photolysis experiments measuring Enro photolysis, assessing ROS production and measuring toxicity under three different light conditions. The distance from the UV lamp to the beaker can be adjusted to vary the irradiation intensities.

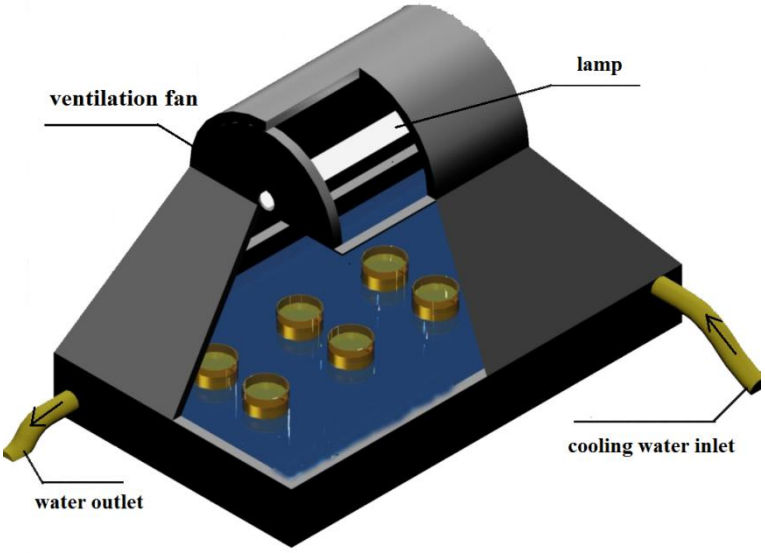

Fig. S1. Experimental schematic of the photolysis experiments under UV light irradiation.

Quantum yield of Enro photolysis under different light conditions

The integral quantum yield is:

$$\Phi = (\text{number of events}) \div (\text{number of photons absorbed}) \quad \text{(S1)}$$

For a photolysis reaction:

$$\Phi = (\text{amount of reactant consumed}) \div (\text{amount of photons absorbed}) \quad \text{(S2)}$$

By this means, the quantum yield of Enro photolysis could be calculated by the light intensity and the decomposed Enro concentrations. The respective light intensities of UV-254, UV-365 and solar in the centre of the reactive solutions were 19.2, 14.0 and ~6.0–7.3 mW cm^{-2}. The energy of a photon is given by the equation:

$$E = h\,c \div \lambda \quad \text{(S3)}$$

The irradiation area of the photolysis reactor was 15.9 cm^2. After irradiation for 30 min, 99.8, 99.4 and 93.8% Enro reduction respectively occurred at initial concentration of 10 mg L^{-1} under light conditions of UV-254, UV-365 and solar. The respective amount of photons absorbed was 7.04×10^{20}, 7.42×10^{20} and $(\sim 3.43–4.18) \times 10^{20}$ under UV-254, UV-365 and solar irradiation. The respective amount of reactant consumed was 3.34×10^{18}, 3.32×10^{18} and 3.14×10^{18} under UV-254, UV-365 and solar irradiation. Thus the respective quantum yield was 0.47, 0.45 and ~0.75–0.92% under UV-254, UV-365 and solar irradiation.

Effect of NO_3^- on Enro photolysis kinetics

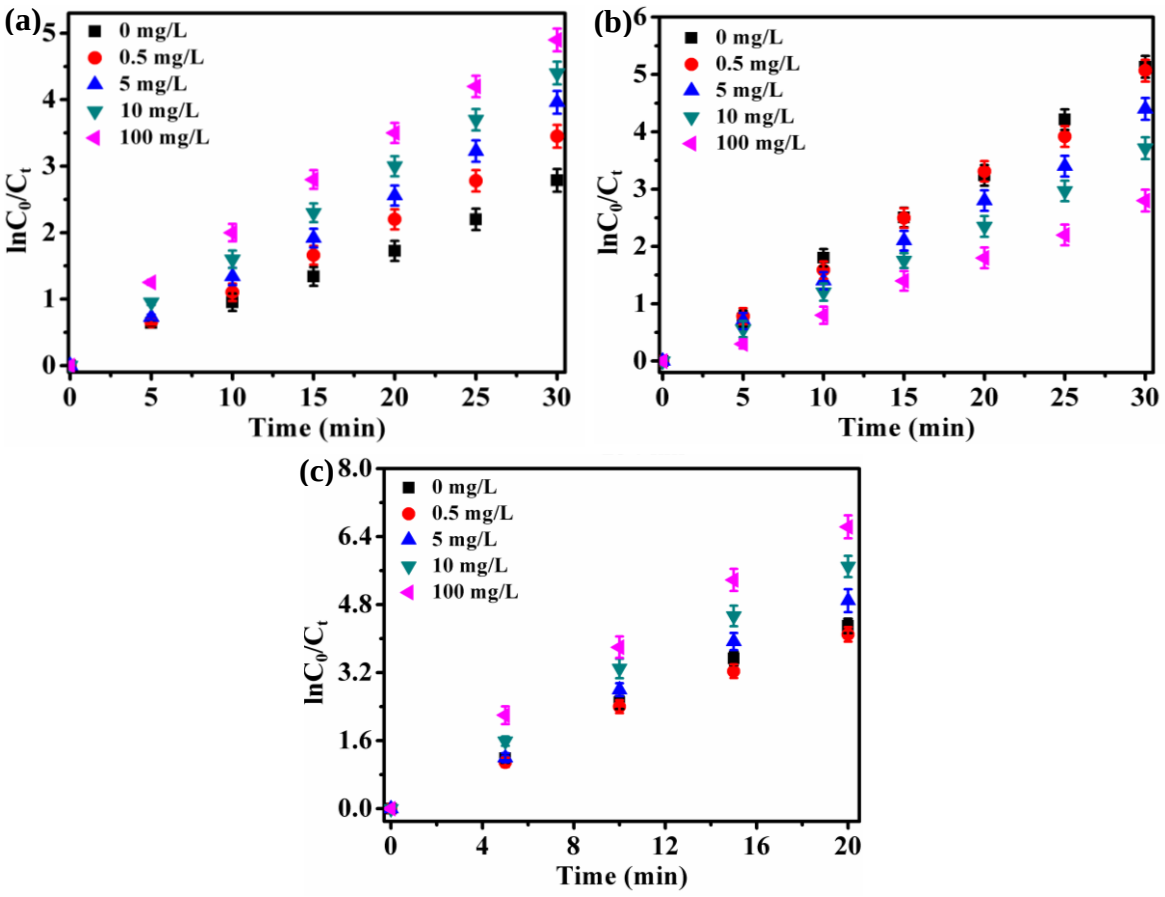

Fig. S2. Effect of NO_3^- on Enro photolysis kinetics under different light irradiation conditions (a) solar, (b) UV-365, (c) UV-254 at pH = 7.1 and initial Enro concentration of 10 mg L^{-1}.

UV-Vis absorption spectrum of aqueous solution of sodium nitrate

The UV-Vis absorption spectrum of sodium nitrate in DI water is shown in Fig. S3. The absorption spectrum of sodium nitrate contains one bond in the wavelength region of ~250–370 nm, which was consistent with previous study reported by Otten et al.[1]

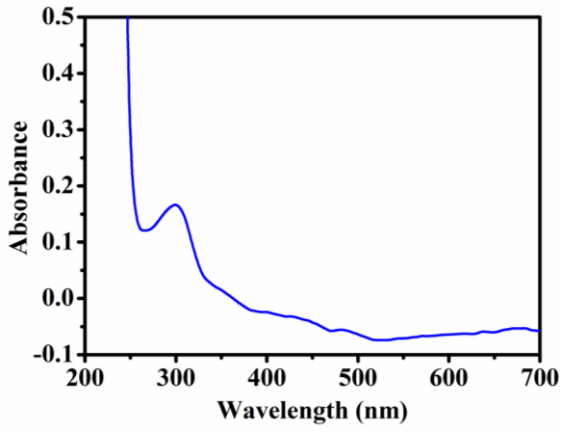

Fig. S3. UV-Vis absorption spectrum of sodium nitrate in DI water.

Primary phototransformations and subsequent reactions of nitrate upon light irradiation

$$NO_3^- + H_2O + h\nu \rightarrow NO_2^{\bullet} + \cdot OH + OH^- \text{ (S4)}$$

$$NO_3^- + h\nu \rightarrow NO_2^- + O\,(^3P) \text{ (S5)}$$

$$NO_2^- + H_2O + h\nu \rightarrow NO\cdot + \cdot OH + OH^- \text{ (S6)}$$

$$NO_2^- + \cdot OH \rightarrow NO_2^{\bullet} + OH^- \text{ (S7)}$$

$$2NO_2^{\bullet} \rightarrow N_2O_4 \text{ (S8)}$$

Detection of ROS in aqueous solution of sodium nitrate

To elucidate the underlying photolysis mechanism of Enro in the presence of nitrate, ESR was conducted to detect ROS in the sodium nitrate solution upon light irradiation. In this study the nitrate solution was excited in ESR cavity by 254 and 532 nm. As shown in Fig. S4, four characteristic peaks of the DMPO–$O_2^{\bullet-}$ spin adducts could be detected under light irradiation (254 and 532 nm) whereas no such signal was detected without direct light irradiation, which indicated that $O_2^{\bullet-}$ was generated upon irradiation of sodium nitrate solution. No appreciable signals of TEMP–$^1O_2$ and DMPO–•OH spin adducts were detected in sodium nitrate solution under irradiation, which indicated that no detectable amounts of $^1O_2$ and •OH were generated in sodium nitrate solution. Despite failure to detect •OH in nitrate solution by ESR, $O_2^{\bullet-}$ dismutation can generate H_2O_2, which can be decomposed to •OH under irradiation.[2] DMPO and TEMP in the absence of sodium nitrate were irradiated while no signals were detected, which indicated that DMPO, TEMP and water could hardly initiate any ROS generation.

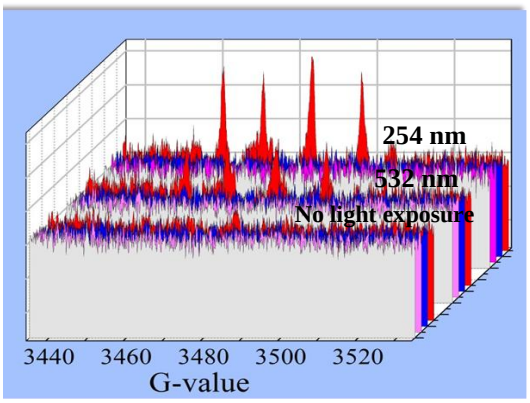

Fig. S4. ESR spectra recorded at ambient temperature of nitrate for DMPO–$O_2^{\bullet-}$ in red, TEMP–$^1O_2$ in blue, DMPO–•OH in pink and control in white.

S7. Effect of HA on Enro photolysis

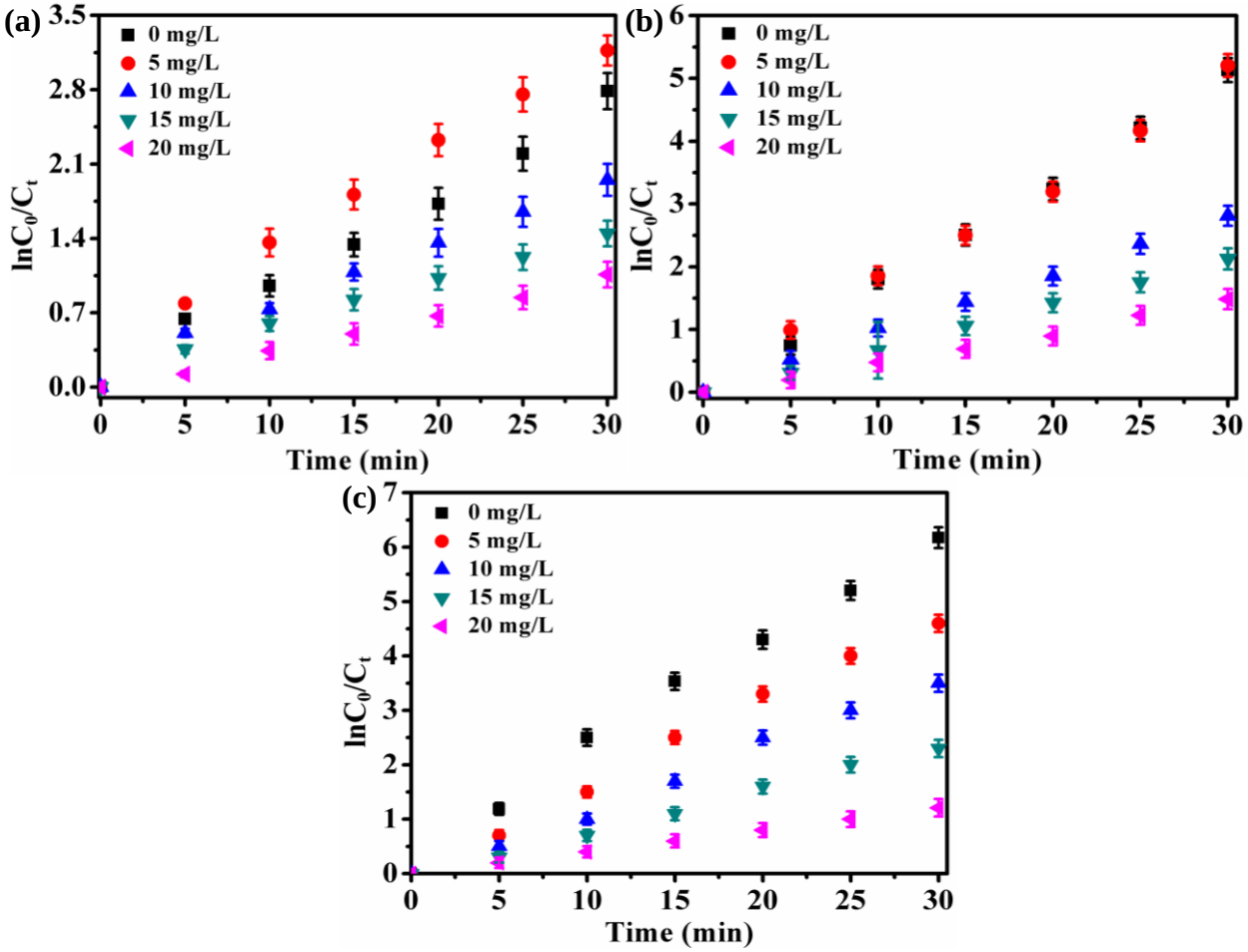

Fig. S5. Effect of HA on Enro photolysis kinetics under different light irradiation conditions (a) solar, (b) UV-365, (c) UV-254 at pH = 7.1 and initial Enro concentration of 10 mg L^{-1}.

Detection of ROS in aqueous solution of HA

To elucidate whether HA can act as photosensitiser, ESR technique was conducted to investigate the photogenerated ROS in the aqueous solution of HA. As shown in Fig. S6, no DMPO–$^1O_2$ spin adducts was detected with or without light irradiation of HA, which indicated that $^1O_2$ was not produced in the aqueous solution of HA. However, six characteristic peaks of the DMPO–$O_2^{\bullet-}$ spin adducts could be found under light irradiation, whereas no such signal was detected without direct light irradiation, which indicated that $O_2^{\bullet-}$ was produced in the aqueous solution of HA. Moreover, four characteristic peaks of the DMPO–•OH species, a 1:2:2:1 quarter pattern, were clearly found with light irradiation whereas no such signal was detected without direct irradiation, which indicated that •OH was generated in the aqueous solution of HA. In conclusion, both $O_2^{\bullet-}$ and •OH was generated in aqueous solution of HA upon light irradiation.

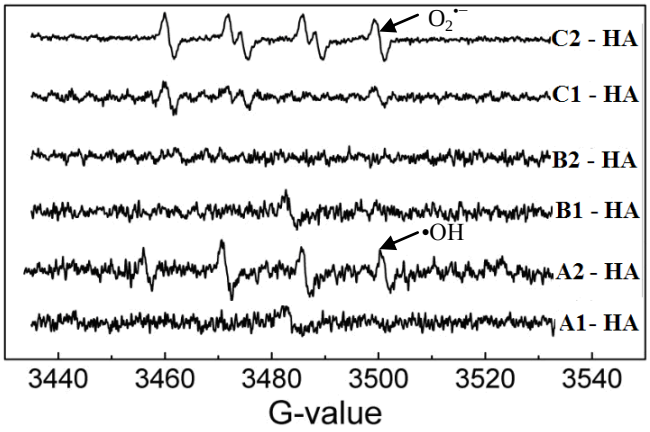

Fig. S6. ESR spectra of the HA aqueous solution recorded at ambient temperature for (A1) DMPO–•OH without direct irradiation, (A2) DMPO–•OH under irradiation of 532 nm, (B1) TEMP–$^1O_2$ without direct irradiation, (B2) TEMP–$^1O_2$ under irradiation of 532 nm, (C1) DMSO–$O_2^{\bullet-}$ without direct irradiation, (C2) DMSO–$O_2^{\bullet-}$ under irradiation of 532 nm.

UV-Vis absorption spectrum of aqueous solution of HA

As shown in Fig. S7, the UV-Vis absorbance of HA decreases monotonically with increasing wavelength. The absorbance determined at wavelength less than 250 nm is much higher than determined at longer wavelength and causes a sharp slope at the shorter wavelength (< 300 nm). This phenomenon was also observed by many previous studies.[3–5] The absorbance at longer

wavelength (>400 nm) is relatively low as compared with those observed at UV and sub-UV ranges (~200–400 nm).

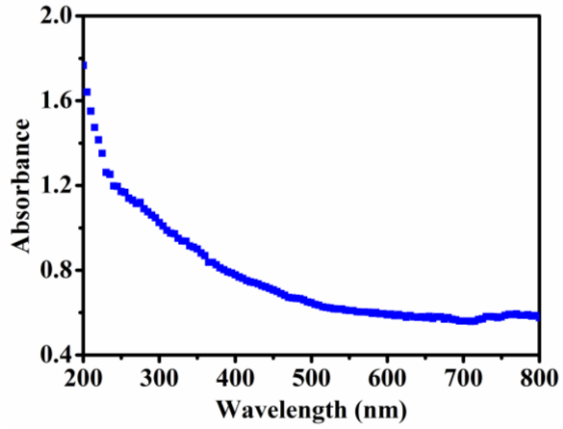

Fig. S7. UV-Vis absorption spectra of HA in DI water.

MS-MS spectra of the photolysis products

The MS-MS spectra for Enro photolysis products under different light conditions are shown in Fig. S8. MS-MS spectra showed F, cyclopropane or ethyl were abstracted from the ions at *m*/*z* 316.3 (1), 332.1 (2) and 374.1 (4) during Enro fragmentation. The ion at *m*/*z* 301.2 (3) obtained by MS-MS spectrum showed the abstraction of COOH and ethyl during Enro fragmentation. MS-MS spectrum showed F and CO_2 were abstracted from the ion at *m*/*z* 263.1 (5) during Enro fragmentation. The ion at *m*/*z* 268.1 (6) obtained by MS-MS spectrum showed the abstraction of H_2O and CO_2 during Enro fragmentation. The ion at *m*/*z* 226.2 (7) obtained by MS-MS spectrum showed the abstraction of CO_2 during Enro fragmentation. The ion at *m*/*z* 230.1 (8) obtained by MS-MS spectrum showed the abstraction of H_2O during Enro fragmentation.

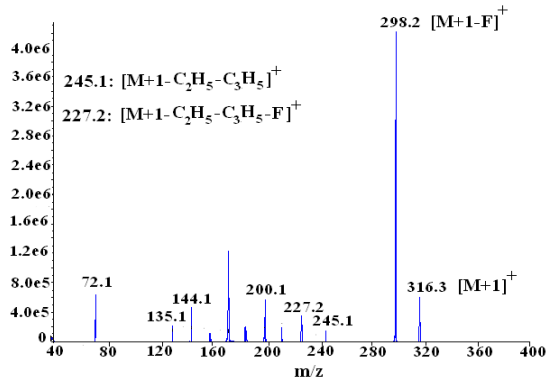

(1) ESI(+)MS-MS (parent ion *m*/*z* 316.3)

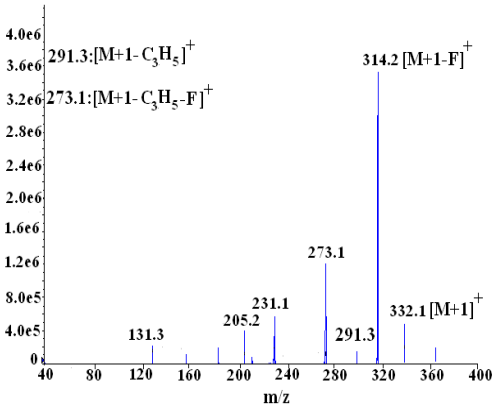

(2) ESI(+)MS-MS (parent ion *m*/*z* 332.1)

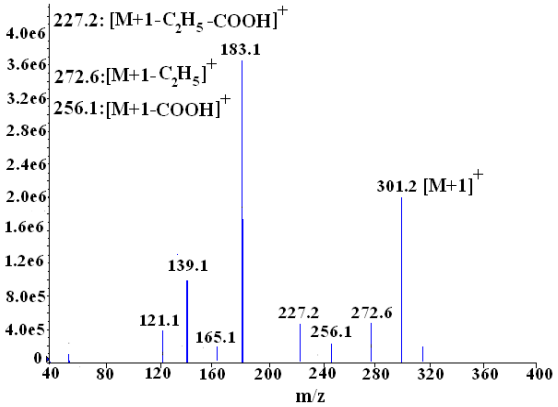

(3) ESI(+)MS-MS (parent ion *m*/*z* 301.2)

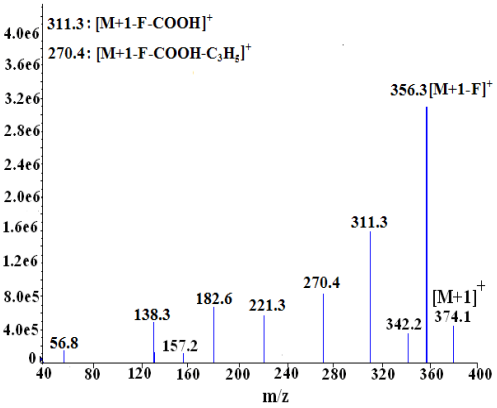

(4) ESI(+)MS-MS (parent ion *m*/*z* 374.1)

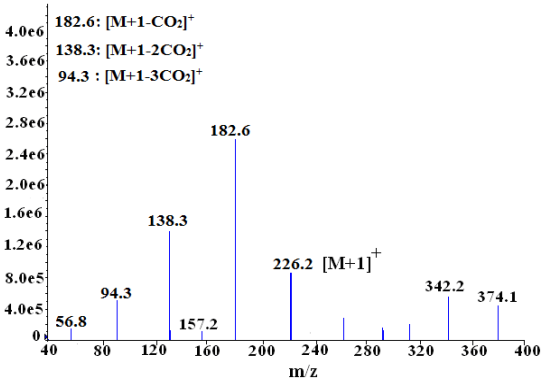

(5) ESI(+)MS-MS (parent ion *m*/*z* 226.2)

Fig. S8. MS-MS spectra for Enro photoproducts under different light conditions. Note that the products 1–4 were under irradiation of solar, UV-365 or UV-254; products 5–7 were only under irradiation of UV-365 and UV-254. The parent ions correspond to the pseudomolecular peak ions $[M+H]^+$.

References

[1] D. E. Otten, P. B. Petersen, R. J. Saykally, Observation of nitrate ions at the air–water interface by UV-second harmonic generation. *Chem. Phys. Lett.* **2007**, *449*, 261. doi:10.1016/j.cplett.2007.10.081.

[2] C. Li, N. Y. Gao, L. Y. G. Wang, Hydrogen peroxide-assisted low pressure UV photodegradation of atrazine in aqueous solution. *Int. J. Environ. Stud.* **2012**, *69*, 625. doi:10.1080/00207233.2012.674780.

[3] R. Duarte, E. B. H. Santos, A. C. Duarte, Spectroscopic characteristics of ultrafiltration fractions of fulvic and humic acids isolated from an eucalyptus bleached Kraft pulp mill effluent. *Water Res.* **2003**, *37*, 4073. doi:10.1016/S0043-1354(03)00411-1.

[4] A. I. Gomes, J. C. Santos, V. J. P. Vilar, R. A. R. Boaventura, Inactivation of bacteria *E. coli* and photodegradation of humic acids using natural solar. *Appl. Catal. B* **2009**, *88*, 283. doi:10.1016/j.apcatb.2008.11.014

[5] G. S. Wang, S. T. Hsieh, Monitoring natural organic matter in water with scanning spectrophotometer. *Environ. Int.* **2001**, *26*, 205. doi:10.1016/S0160-4120(00)00107-0.